Green Chemistry

Accepted Manuscript

ROYAL SOCIETY OF CHEMISTRY

www.rsc.org/greenchem

A Process for Desulfurization of Coking Benzene by a Two-step Method with Reuse of Sorbent/Thiophene and Its Key Procedures

Junjie Liao, Yashan Wang, Liping Chang, Weiren Bao*

State Key Laboratory Breeding Base of Coal Science and Technology Co-founded by Shanxi Province and the Ministry of Science and Technology, Taiyuan University of Technology, Taiyuan 030024, Shanxi, PR China

Abstract: Pure benzene is an important chemical feedstock, and coking benzene is one of its sources. However, the industrialized coking benzene refining processes are not green and sustainable. To solve this problem, a green two-step process for the desulfurization of coking benzene with the advantages of easy operation, low environmental pollution and solid waste (sorbent/thiophene) recyclability was evaluated. The thiophene in coking benzene was firstly alkylated by the olefins present in it by a suitable $AlCl_3$/silica gel catalyst to produce alkylthiophenes, which can be easily separated by distillation. $AlCl_3$/silica gel catalyst obtained by a novel green process was effective in catalyzing the alkylation of thiophene by 1-hexene with an efficiency of removing thiophene up to 94.2%. $AlCl_3$ was grafted on silica gel by reacting with hydroxyls on its surface, which could prevent the dissolution problem of $AlCl_3$ in benzene. The residual thiophene with its concentration range of 100-1000 mg/L in benzene was then almost completely removed by adsorption using an ion-exchanged zeolite. The CeY zeolite sorbent showed excellent performance in deeply removing residual thiophene in the benzene, in which the adsorption desulfurization over CeY sorbent fits a Langmuir isotherm. The product met the requirements for a chemical feedstock, in that no thiophene was measured in the purified benzene by gas chromatography with flame photometric detector, could be given. The CeY zeolite with

*Corresponding author: Weiren Bao; E-mail: baoweiren@tyut.edu.cn; Fax: +86 351 6010482; Tel: +86 351 6010482.

adsorbed thiophene was used to prepare polythiophene-CeY composites by chemical oxidative polymerization using anhydrous $FeCl_3$ as oxidant at 0 °C. The decomposition temperature of the polythiophene-CeY composites is 480 °C, which is 60 °C higher than that of polythiophene.

Keywords: desulfurization; thiophene; adsorption; alkylation; polythiophene-CeY composite

1. Introduction

Retention of sulfur compounds in chemical feedstocks and liquid fuels is a potentially important source of sulfurous pollutants. So much attention has been directed to desulfurization processes[1-6]. However, most of these concern the desulfurization of liquid fuels[1-5], and much less work has been done on desulfurization of other hydrocarbons, especially aromatics.

Pure benzene is an important chemical feedstock, usually produced by refining coking benzene and petroleum benzene, which are byproducts of the coking and petrol industries respectively. In China, coking benzene production makes up about 40%~50% of the total amount of crude benzene produced[7]. However, currently about 20% of the pure benzene produced in China is obtained from coking benzene[7], because some of the impurities present are difficult to remove. The phenols, olefins (mainly 1-hexene, 1-pentene and styrene), are not a serious problem, but the sulfur-containing impurity thiophene (about 0.5wt% of the crude benzene[8]) is difficult to remove on account of its physicochemical similarity to benzene, and its concentration must be minimized to avoid catalyst poisoning and environmental pollution. For instance, benzene to be used as feedstock for cyclohexanone-oxime production must contain less than 0.01 ppm thiophene. Separated thiophene is not a waste product but can be used in the synthesis of e.g. dyes, pharmaceuticals, pesticides, polymers. A derivative of thiophene, polythiophene, which has high electrical conductivity and photoelectric conversion, has attracted widespread attention in recent years for applications in solar cells[9, 10], chemical sensors[11], luminescent transistors[12] and luminescent materials[13, 14]. Moreover, some of the

useful properties of polythiophene can be improved significantly by coupling with inorganic materials, such as zeolites[15, 16], Al_2O_3[17], ZnO[18, 19], silica[20] and active carbon[21].

Current industrialized processes for refining and desulfurizing coking benzene include sulfuric acid washing, catalytic hydrogenation and extractive distillation. In sulfuric acid washing, the coking benzene is washed with 93%~95% sulfuric acid, which reacts with the thiophene to produce thiophene sulfonate, soluble in the sulfuric acid[8]. This process has the advantage of low operating costs, but many disadvantages, including equipment corrosion, the pollution caused by the waste acid and low desulfurization efficiency[22]. During the catalytic hydrogenation process, the thiophene and the olefins, another impurity in the crude benzene, react with H_2 to produce H_2S and alkanes at high temperature and pressure over catalyst. The efficiency of removing thiophene by this method is relatively high, but the consumption of H_2 and energy is also high[23]. The sulfuric acid washing and catalytic hydrogenation methods do not isolate the thiophene, but transform it into relatively useless pollutants (thiophene sulfonate, H_2S) and the residual thiophene concentration in benzene is still generally higher than the required standard of < 0.01 ppm due to mass transfer limitations. The extractive distillation method, which was first commercialized in 2008[24], also can not remove the thiophene from benzene to below the 1 ppm level, and the energy consumption is high due to the large amount of extracting agent used in this process[7].

Recently, Sinopec and Philips have invented a new desulfurization catalyst S-sorb[25]， in which the catalyst is claimed to remove 99+% of sulfur-containing compounds by catalytic hydrogenation. After this desulfurization process, the thiophene concentration in the product is in the range of 6-10 ppm[26], which is still much too high for the benzene to be used as feedstock for cyclohexanone production etc. For such purposes, a sulfur concentration of less than 0.01 ppm is required. Furthermore, for this process, the very valuable thiophene is transformed into SO_2 after the catalyst regeneration[25].

Therefore, it is necessary to find a new method for refining and desulfurizing coking benzene which can meet the very strict requirements of chemical synthesis and isolate the thiophene or useful thiophene derivatives to be recycled. For this purpose, in this paper, a green two-step process for the desulfurization of coking benzene with the advantages of easy operation, low environmental pollution and solid waste (sorbent/thiophene) recyclability was outlined and tested.

2. Description of the Proposed Process of Coking Benzene Desulfurization

The process chart of the proposed novel desulfurization method for coking benzene, which has been verified by preliminary tests described in this paper, is shown in **Figure 1**. The main steps in the process are two-step removal of thiophene and synthesis of polythiophene-zeolite composite materials.

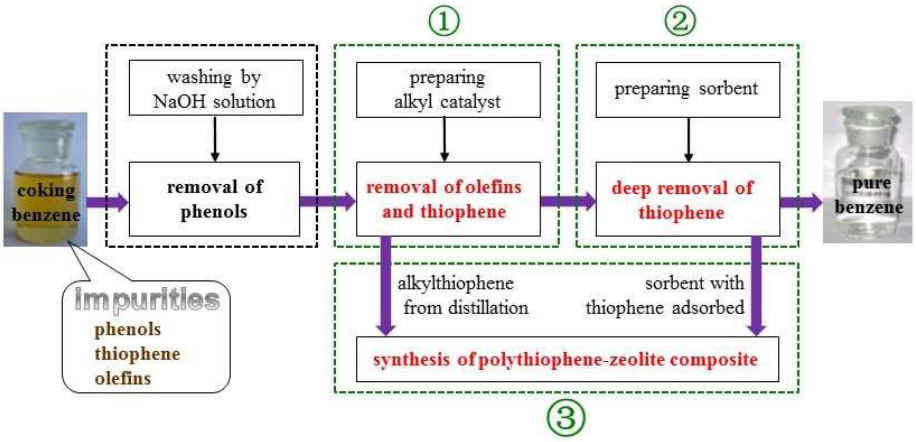

Figure 1. Process chart for desulfurization of coking benzene and recycle of thiophene and used sorbent

The process can be summarized as follows. As a first step, the coking benzene is washed with aqueous sodium hydroxide solution to remove the phenols, an important impurity in benzene. In the second step, the olefins and most of the thiophene in the crude benzene are catalytically converted to alkylthiophenes at atmospheric pressure and low temperature. The alkylthiophenes can be easily separated by distillation because of their significantly different

boiling points from that of benzene. In the third step, the residual thiophene in the benzene is almost completely removed by adsorption on ion-exchanged zeolite at atmospheric pressure and room temperature. After deep desulfurization, the pure benzene produced satisfies the specifications for a chemical-synthesis feedstock. Finally, in the fourth step, the zeolite-adsorbed thiophene and the alkylthiophenes isolated are used to prepare polythiophene-zeolite composite materials. Three of the four steps are the subject of our experiments. The first step, phenol removal, was commercialized some years ago[8].

The challenges for this process are to find a good method for the $AlCl_3$ loaded catalyst preparation, to prepare a sorbent for the selective removal of thiophene from benzene to less than 0.01 ppm and to optimize the operation parameters and finally, to synthesize polythiophene/zeolite composite by using the recycled alkyl thiophene and sorbent with thiophene adsorbed.

2.1. Catalyst preparation and catalytic alkylation of thiophene

For the alkylation method, the alkyl catalyst always used is $AlCl_3$, which is an effective Friedel-Crafts alkylation catalyst in the chemical industry. However, it has not been employed for the desulfurization of coking benzene because it is slightly soluble in coking benzene and hence erodes steel equipment and is difficult to separate from product. Thus, to use $AlCl_3$ in a coking benzene medium, it is necessary to load the anhydrous $AlCl_3$ on a carrier. The method of loading $AlCl_3$ on the carrier is the most important factor in determining whether this reaction can be carried out cheaply and expeditiously with minimum waste. The main loading methods reported in the literature are the gas loading method[27] and the impregnation method[28]. In the gas loading method, the carrier is treated in the fixed bed with $AlCl_3$ vapor carried by the gas, so that $AlCl_3$ is wasted, and the loading process is lengthy. In the impregnation method, the carrier is impregnated with an anhydrous liquid medium (e.g. CS_2, CCl_4), in which the $AlCl_3$ is dissolved. The anhydrous liquids used are all volatile toxic organic

substances and the impregnated sample must be filtered and calcined to remove the liquid medium, so this method has the disadvantages of environmental pollution and cumbersome preparation steps. To avoid the shortcomings of previous methods as discussed in the introduction section, a novel loading method was devised, in which the catalyst was prepared under high pressure (**Figure 2**). Anhydrous $AlCl_3$ powder and silica gel (1.5~2.5 mm) were selected as the active component and carrier respectively based on the results of screening tests. 2.0 g of $AlCl_3$ was put on the bottom of the autoclave, which had a teflon lining to prevent steel corrosion caused by $AlCl_3$, and 10.0 g of the silica gel which has been calcined at 400 °C for 3 h was put in a teflon basket with 1mm pores over the whole surface. The autoclave was sealed and heated in a muffle furnace at 180 °C for 4 h. The temperature was chosen because the sublimation temperature of $AlCl_3$ is 178 °C so that it can be uniformly loaded on silica gel when the loading temperature is 180 °C or higher. The autoclave was taken out and cooled in air, and the catalyst was then taken out. The major advantages of this method are the high loading of $AlCl_3$ on the carrier and no escape of caustic $AlCl_3$ during the preparation of catalyst. The utilization efficiency of $AlCl_3$ (ω_{AlCl_3}, %) is defined by **equation (1)**, and the active component content (c_{ac}, %) was calculated by **equation (2)**.

$$\omega_{AlCl_3} = \frac{m_{catalyst} - m_{carrier}}{m_{AlCl_3}} \times 100\% \quad (1)$$

$$c_{ac} = \frac{m_{catalyst} - m_{carrier}}{m_{catalyst}} \times 100\% \quad (2)$$

where, $m_{catalyst}$ is the weight of the prepared $AlCl_3$/silica gel catalyst (g); $m_{carrier}$ is the weight of silica gel carrier used (g); m_{AlCl_3} is the weight of $AlCl_3$ used.

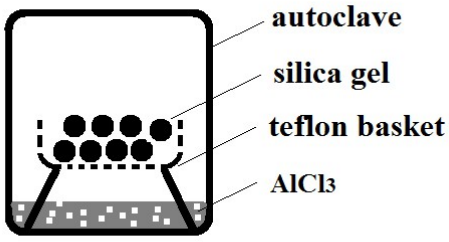

Figure 2. Schematic diagram of the apparatus used for the preparation of $AlCl_3$/silica gel catalyst

The alkylation reaction between thiophene and olefin was carried out in a simulated coking benzene solution which had a thiophene concentration of 704.5 mg/L and a molar ratio of 1-hexene to thiophene of 6:1. The experimental apparatus is shown in **Figure 3**. In the experiment, 5.0 g $AlCl_3$/silica gel catalyst was added to 100 mL simulated coking benzene solution in a flask under reflux, and the mixture was heated with stirring in a silicone oil bath at 65 °C for 4 h. After the reaction, the concentrations of thiophene and 1-hexene in the solution were determined by gas chromatography with flame photometric detector (GC-FPD)[29] and flame ionization detector (GC-FID), respectively, and the alkylation products were qualitatively analyzed by GC-MS (HP 6890-5973MSD). The GC-FPD used in this study is GC-950 (Shanghai Haixin chromatography Co., Ltd.) with TCEP-7 column (2.5 m × ϕ4 mm), in which the column oven temperature, injection temperature and detector temperature are 80 °C, 120 °C and 160 °C, respectively. The carrier gas is high purity nitrogen with the column pressure of 0.1 Mpa. The flow rate of high purity hydrogen and air is respectively 40 mL/min and 50 mL/min. The GC-FID (Shanghai Tianmei chromatography Co., Ltd.) and the GC-MS are all coupled with 30 m length of capillary columns (HP-5MS). The carrier gas is He with a flow rate of 0.6 ml/min, and the column oven temperature, injection temperature and detector temperature are 60 °C, 200 °C and 200 °C, respectively. The efficiency of thiophene removal (η, %) was calculated by **equation (3)**.

$$\eta_{thiophene} = \frac{c_o - c}{c_o} \times 100\% \quad (3)$$

where, c_o and c is the concentration (mg/L) of thiophene in the solution before and after alkylation reaction, respectively.

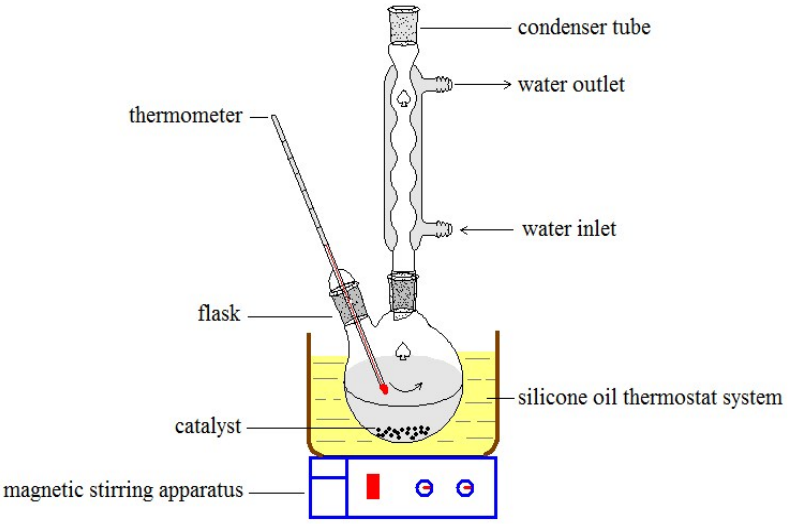

Figure 3. Experimental apparatus for the alkylation of thiophene

2.2. Sorbent modification and deep removal of thiophene

Several papers have been published by our group and others on the adsorption desulfurization of coking benzene by using suitable sorbents, such as modified ZSM-5 zeolite[30-33], modified MCM-41 zeolite[34], nickel based amorphous alloy[35] and modified γ-Al_2O_3[36] and SiO_2[37]. However, these sorbents could not remove enough of the thiophene from benzene to give the required low sulfur concentration. Compared with other sorbents which have been trialed for adsorption desulfurization from coking benzene, Y-type zeolite has many properties which make it more useful sorbent for molecular separation including uniform size pores, large surface area, good thermal stability and strong adsorption selectivity[38]. Thus, NaY zeolite with a Si/Al ratio of 5:1 and particle size of 0.2~0.3 mm was selected as the precursor of the sorbent for thiophene removal and Ce^{4+}, Ni^{2+}, Zn^{2+} or Ag^{+} as nitrate solutions (10 mL solution per gram NaY zeolite) were ion-exchanged into zeolite samples at 100 °C under reflux. The

samples were exhaustively washed by de-ionized water, dried in an oven at 120 °C overnight, calcined at 700 °C for 2 h, and the ion-exchange process as above was repeated to reach a higher metal ion loading. The ion-exchanged sorbent so obtained is denoted MY where M is the metal.

A static adsorption experiment was used to select the best sorbent. 1.00 g sorbent was kept in 4.00 mL thiophene-benzene solution with a thiophene concentration of 500.0 mg/L at room temperature and ambient pressure for 24 h, to reach what was assumed to be adsorption quasi-equilibrium. The concentration of thiophene in the solution was then determined by GC-FPD. The removal efficiency of thiophene (η) was calculated following **equation** (**3**). In order to obtain more accurate data, this experiment and the experiment described in section 2.1 were all repeated for another time, and then the average value of the results from the same two experiments was calculated.

Fixed-bed adsorption, closer to a practical process, was used to investigate the deep removal of thiophene from benzene on a larger scale and to optimize to operation parameters. The process chart is shown in **Figure 4**.

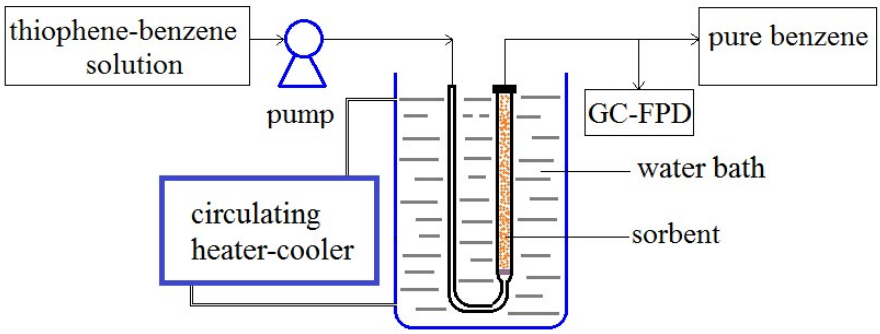

Figure 4. Process chart for thiophene dynamic adsorption in the fixed bed reactor

A glass U-tube 150 mm long with inner diameter 10 mm was used as the fixed-bed reactor. About 6.00 g of the best sorbent was pre-loaded into the reactor. A thiophene-benzene solution was pumped through the sorbent bed from the bottom, with the temperature of the sorbent bed

being controlled by a water bath connected to a circulating heater-cooler, which could hold the temperature at any desired value between 22 °C and 70 °C. The particle size of the sorbent, the flow rate of the thiophene-benzene solution, the bed temperature and the concentration of the thiophene in the solution were all varied, and the effects of these variations were discussed. The concentration of thiophene in the outlet solution was measured by GC-FPD every 3-10 min. The time interval from the beginning to the time at which there was a measurable thiophene concentration (about 0.01 ppm) in the outlet solution was defined as the breakthrough time (t). The thiophene capacity of the CeY sorbent was calculated using **equation** (**4**).

$$Q = \frac{\int_0^t v(c_0 - c)dt}{1000m} \quad (4)$$

where, Q is the thiophene capacity of the sorbent (mg/g); v is the flow rate of the thiophene-benzene solution (mL/min); c_0 and c are the thiophene concentration in the inlet and outlet solution respectively (mg/L); t is the breakthrough time (min); m is the weight of sorbent (g). After adsorption, the sorbent, denoted CeY-T, was taken out and dried in air for further utilization.

2.3. Preparation of polythiophene-Y zeolite composite

The polythiophene-Y zeolite composite was prepared as follows. 5.00 g of thiophene was mixed with 50 mL $CHCl_3$ in a conical flask reactor, which was kept at 0 °C by a thermostat system. Then 10.00 g of the CeY-T (see section 2.2) and 10.00 g of $FeCl_3$ were added. The mixture was stirred for 12 h. The product was then exhaustively washed with anhydrous ethanol, filtered, and the solid was dried in a vacuum oven at 50 °C for 12 h. For comparison, polythiophene was also prepared by the same procedure, except that no CeY-T was added.

2.4. Characterization of samples

The X-ray diffraction (XRD) of $AlCl_3$/silica gel catalyst, CeY zeolite, polythiophene and

polythiophene-CeY samples was measured in a D/max-2500 spectrometer (Rigaku, Japan) at a scanning rate of 5 °/min from 5 ° to 85 ° with Cu-Kα radiation of wavelength 0.154 nm, 40 kV tube voltage and 100 mA tube current. Moreover, before XRD characterization, the samples were all ground into powder.

FT-IR spectra used to characterize the polythiophene-CeY and CeY were recorded on an IR Prestige-21 spectrometer (Shimazu, Japan) in the 400-2000 cm^{-1} wave number range at a resolution of 2 cm^{-1}.

The thermal stability of polythiophene and polythiophene-CeY was determined in a STA409C thermogravimetric analyzer (Netzsch, Germany). The carrier gas was air flowing at 100 mL/min and the test temperature increased from 30 °C to 1000 °C with a heating rate of 10 °C/min.

3. Results and Discussion

3.1. Performance of $AlCl_3$/silica gel catalyst for removing thiophene and olefin from benzene

The utilization efficiency of $AlCl_3$ calculated by **equation** (**1**) with active component content calculated by **equation** (**2**) in $AlCl_3$/silica gel catalyst, prepared under high pressure, is shown in **Figure 5** as a function of temperature. The loading of $AlCl_3$ on silica gel carrier in the sealed, high pressure system is efficient, which implies that very little $AlCl_3$ was lost during the preparation process. The utilization efficiency of $AlCl_3$ reached its maximum, 92.5%, at 220 °C. For comparison, catalyst was also prepared by the gas loading method[27] (section 2.1), for which the maximum utilization efficiency was less than 70.0%. It should be noted that, though $AlCl_3$ is slightly soluble in coking benzene, after it is loaded on silica gel it will be bonded to the OH groups on the surface[27], which would inhibit its dissolution. Thus no corrosion problems are anticipated. Compared to the gas loading method, loading was rapid and efficient and no toxic solvents were required, unlike the impregnation method.

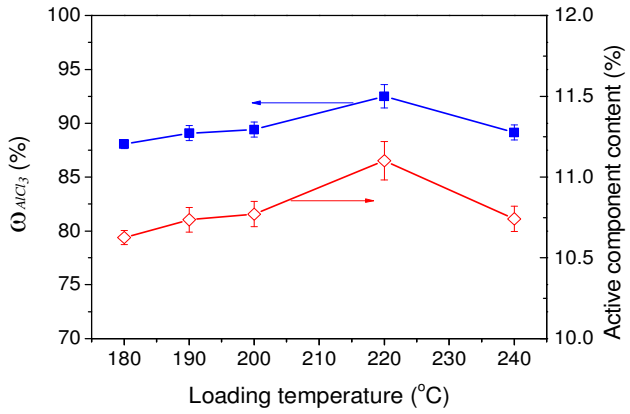

Figure 5. Utilization efficiency and active component content of $AlCl_3$ on $AlCl_3$/silica gel catalysts prepared at different temperatures

Figure 6 shows the XRD patterns of $AlCl_3$/silica gel catalyst, silica gel carrier and anhydrous $AlCl_3$. The XRD pattern of $AlCl_3$/silica gel catalyst was similar to that of the silica gel carrier and no anhydrous $AlCl_3$ peaks were observed, which indicates that the active component species were well dispersed. Because the active component content at different temperatures was always higher than 10.5% (**Figure 5**), well defined crystals would easily be detected by XRD if the active component was not well dispersed. Moreover, as reported by literature[27, 39], the $AlCl_3$ could graft on silica gel by the reaction of between $AlCl_3$ and hydroxyls on the surface, as shown in **Figure 7**. This kind of combination can prevent the dissolution problem of $AlCl_3$ in benzene.

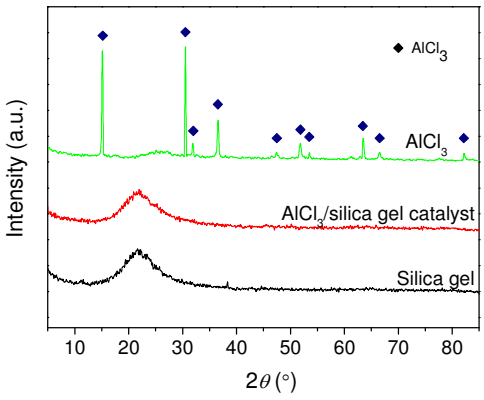

Figure 6. XRD patterns of $AlCl_3$/silica gel catalyst

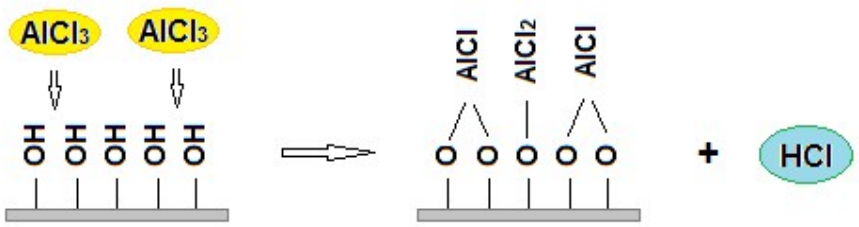

Figure 7. Scheme of the grafting of $AlCl_3$ on the surface of silica gel

Figure 8 shows the efficiency of thiophene removal from benzene with and without 1-hexene for the $AlCl_3$/silica gel catalyst. The $AlCl_3$/silica gel catalyst removed 36.7% of the thiophene from benzene even without the addition of 1-hexene, attributable to the attraction of the Lewis base thiophene to the Lewis acid $AlCl_3$. This attraction is in agreement with the principle of "Hard and Soft Acids and Bases" implied by Lewis electron theory[40]. Adding 1-hexene to the benzene solution greatly increased the removal efficiency of thiophene, to a maximum level of 94.2%, which is much higher than that obtained by previous work[27]. Furthermore, the evaluation conditions (section 2.1), for the $AlCl_3$/silica gel, imply that 20 L of solution can be treated by one kg of catalyst. No 1-hexene was measured by GC-FID, which suggests that the $AlCl_3$/silica gel catalyst prepared by the above method had good catalytic activity for the simultaneous removal of thiophene and 1-hexene by alkylation. The GC-FPD chromatograms of the solutions with and without 1-hexene after reaction are shown in **Figure 9(a)**. The thiophene peak is clearly weaker and a new peak at retention time 13.5 min appears in the chromatograms of the product solution when the original solution contained 1-hexene. Qualitative GC-MS analysis was undertaken to assign the peak (see **Figure 9(b)** and **Table 1**). The presence of 2-hexylthiophene and 2-isohexylthiophene is clear evidence for the significant alkylation of thiophene by 1-hexene. Moreover, the appearance of 2-butyl-5-ethylthiophene, 2-propylthiophene and 2, 4-dimethylthiophene with side chains of different length in the products suggests that cracking reactions of 1-hexene accompanied the alkylation reaction. The production of 1-ethylbutylbenzene and 1-methylpentylbenzene

indicates that the $AlCl_3$/silica gel catalyst also catalyzed the alkylation reaction of benzene. However, given that the concentration of thiophene in the mixture was much less than that of benzene, the relative intensity of the substituted thiophene and benzene peaks after alkylation of thiophene-benzene implies that the $AlCl_3$/silica gel catalyst had good catalytic selectivity.

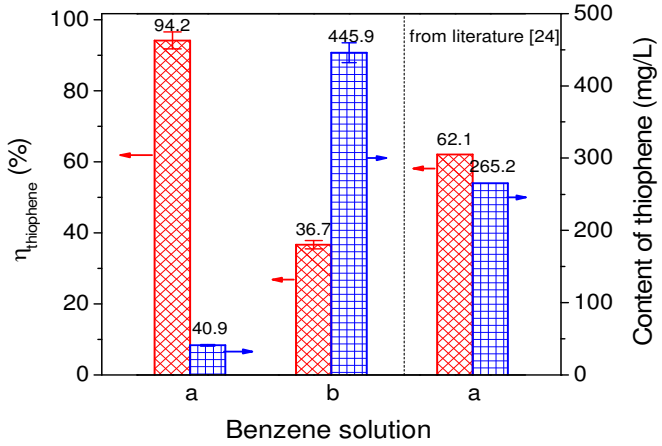

Figure 8. Removal efficiency of thiophene and the thiophene content of the solution after alkylation over $AlCl_3$/silica gel catalyst compared with those of an $AlCl_3/\gamma$-Al_2O_3 catalyst as reported in the literature[27] with (a) and without (b) 1-hexene (initial thiophene content of the benzene solution 704.5 mg/L)

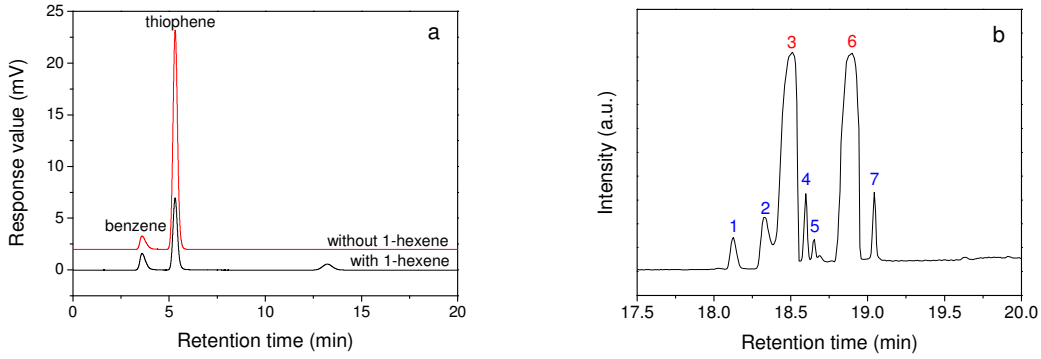

Figure 9. GC-FPD spectra **(a)** of the benzene solutions with and without 1-hexene after removing thiophene and GC-MS spectrum **(b)** of reaction products of thiophene with 1-hexene in benzene

Table 1. Analysis results for the GC-MS spectrum of products from the reaction of 1-hexene with thiophene in benzene

Peak number	Retention time (min)	Substance
1	18.13	2-butyl-5-ethylthiophene
2	18.33	2-hexylthiophene
3	18.51	1-ethylbutylbenzene
4	18.60	2-propylthiophene
5	18.65	2-isohexylthiophene
6	18.90	1-methylpentylbenzene
7	19.04	2,4-dimethylthiophene

3.2. Deep removal of thiophene over modified Y zeolite

3.2.1 Selection of the modified Y zeolite for thiophene removal

The static adsorption results for different sorbents are shown in **Figure 10**. In this Figure, A and B were 15wt% Ag loaded on γ-Al_2O_3 by a conventional and an ultrasound-assisted incipient-wetness impregnation method respectively[36]; C and D were CeZSM-5 and LaZSM-5 sorbent[31]; E was Si-CuZSM-5 sorbent[33]; F gives the highest desulfurization efficiency reported for a nickel based amorphous alloy[35]; G was Ce-MCM-41[34]. The best sorbent was better than even the most efficient one investigated previously[31, 33-36]. The desulfurization efficiency increased when the NaY zeolite was modified by any of the different metal ions used, but the desulfurization efficiency of CeY was clearly the highest. This was probably because CeY sorbent acted by two adsorption mechanisms, π-complexation[41-44] and the formation of specific sulfur-metal bonds between Ce^{4+} and thiophene[44], whereas the other sorbents only adsorbed by π-complexation[41-44]. Since both benzene and thiophene have π bonds, they can both be adsorbed by this mechanism and there will be competition for

adsorption between thiophene and benzene. Thus, if this is the only adsorption mechanism, efficiency for thiophene adsorption will be relatively poor. However, formation of specific sulphur-metal bonds between thiophene and Ce^{4+} will obviously not be possible for adsorption of benzene, so that the efficiency of CeY for thiophene adsorption will be higher than that of the other sorbents.

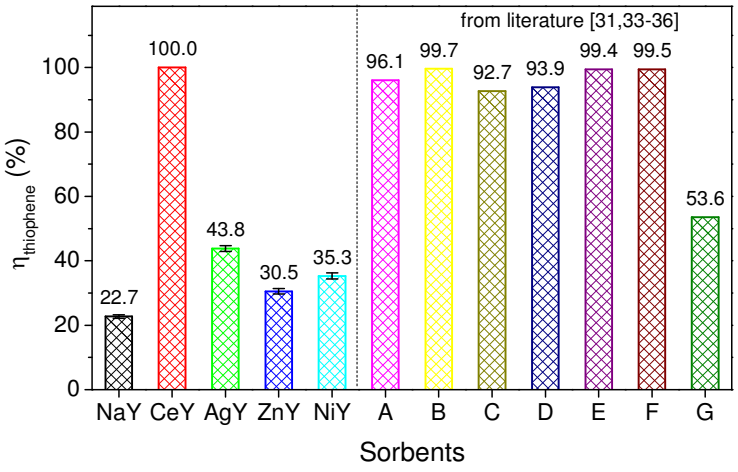

Figure 10. Desulfurization efficiency of different sorbents trialed in this work compared with A-G reported in the literature

3.2.2 Effect of operation parameters on the fixed bed desulfurization behavior of CeY sorbent

Effect of the particle size on the desulfurization behavior of CeY sorbent, when the desulfurization temperature, thiophene concentration and flow rate were 22 °C, 500mg/L and 0.15 mL/min respectively, is shown in **Figure 11** and **Table 2**. Particle size had an obvious effect on the desulfurization behavior of CeY sorbent. The breakthrough time and the adsorption capacity both increased as the average particle size deceased, but the change became small at small particle sizes.

The increase in breakthrough time and adsorption capacity can be explained by the change in internal diffusion resistance and surface area with particle size. Generally, the internal diffusion resistance would be expected to decrease with decreasing particle size and

the surface area of the sorbent increased with decreasing particle size (**Table 3**). Both these changes would lead to an increase in breakthrough time and adsorption capacity

The decrease in the rate of change of breakthrough time and adsorption capacity with particle size at small particle sizes can be explained by the increase in packing density with decrease in particle sizes. This will decrease the height of the sorbent bed and therefore increase the space velocity (**Table 3**), which will lead to a shortening of the residence time of the thiophene in the sorbent bed at low particle size. This will tend to decrease the breakthrough time and adsorption capacity and will partly counteract the favorable effects of decreasing particle size, particularly at low average particle sizes. Taking into account the change in the pressure drop and the energy consumption with particle size, it was concluded that the particle size 0.2-0.3 mm was optimum.

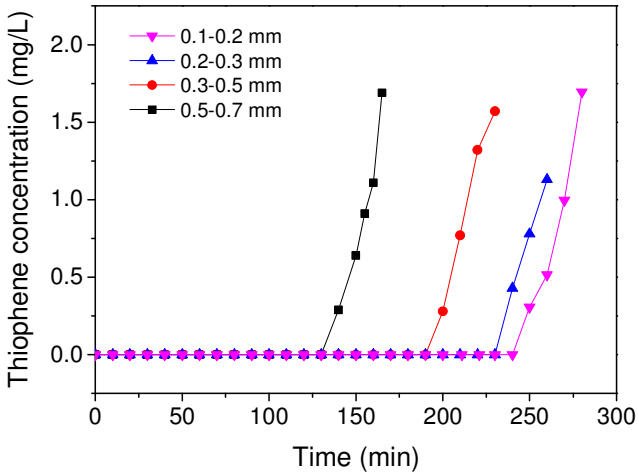

Figure 11. Breakthrough curves of CeY sorbents with different particle size

Table 2. Adsorption capacity of CeY sorbents with different particle size

Range of particle size (mm)	0.5-0.7	0.3-0.5	0.2-0.3	0.1-0.2
Q (mg/g)	1.63	2.38	2.88	3.01

342 **Table 3.** Pore structure parameters of series of CeY sorbents with different particle size and
343 the corresponding operation parameters

Particle size (mm)	S_{BET} (m^2/g)	Packing density (g/mL)	Space velocity (h^{-1})
0.1-0.2	441	0.6554	0.874
0.2-0.3	424	0.6339	0.845
0.3-0.5	418	0.6220	0.827
0.5-0.7	403	0.6122	0.816

344

345 Effect of the flow rate of the thiophene-benzene solution on the desulfurization behavior of
346 CeY sorbent, when the desulfurization temperature, thiophene concentration and sorbent
347 particle size were 22 °C, 500 mg/L and 0.2-0.3 mm respectively, is shown in **Figure 12**, and
348 the corresponding adsorption capacities are shown in **Table 4**. As the flow rate increased from
349 0.10 mL/min to 1.00 mL/min, the breakthrough time decreased. At low flow rates, the
350 adsorption capacity was practically independent of flow rate, but above a flow rate of 0.15
351 mL/min, the adsorption capacity decreased with increasing flow rate. Two parameters
352 affecting the adsorption capacity will change with flow rate. The external diffusion resistance
353 will decrease with increasing flow rate, which will tend to increase the adsorption capacity
354 and the residence time of the solution in the sorbent bed will also decrease with increasing
355 flow rate, which will tend to decrease the available adsorption time, and hence the adsorption
356 capacity. The results imply that the second factor is more important than the first for the range
357 of flow rates investigated. The results indicated that 0.15 mL/min was the optimum flow rate,
358 in that the amount of solution desulfurized in a given time was a maximum for the highest
359 adsorption capacity.

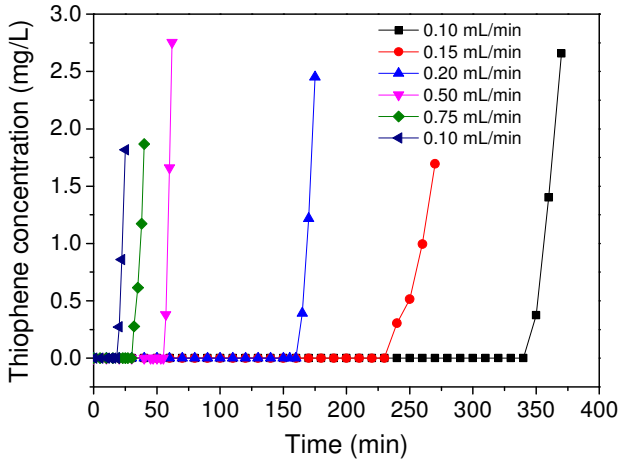

Figure 12. Breakthrough curves of CeY sorbent for different solution flow rates

Table 4. Adsorption capacity of CeY sorbent for different solution flow rates

Flow rate (mL/min)	0.10	0.15	0.20	0.50	0.75	1.00
Q (mg/g)	2.84	2.88	2.67	2.29	1.88	1.50

The effect of adsorption temperature on the desulfurization, when the particle size, thiophene concentration and flow rate were 0.2-0.3 mm, 500 mg/L and 0.15mL/min respectively, is shown in **Figure 13** and **Table 5**. When the temperature increased from 22 °C to 70 °C, both the breakthrough time and adsorption capacity decreased. Adsorption of thiophene was probably due to a combination of physical and chemical adsorption, and there would be a decrease of physical adsorption capacity and hence decreased totally adsorption capacity at higher temperatures. Thus in the temperature range of 22 °C to 70 °C, 22 °C was the best temperature for desulfurization.

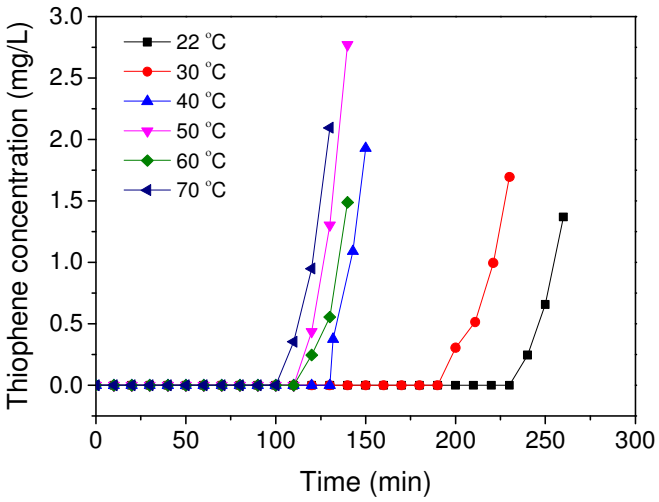

Figure 13. Breakthrough curves of CeY sorbent at different bed temperatures

Table 5. Adsorption capacity of CeY sorbent at different bed temperatures

Bed temperature (°C)	22	30	40	40	60	70
Q (mg/g)	2.88	2.38	1.63	1.38	1.40	1.24

3.3. Polythiophene-zeolite composite

FT-IR characterization was used to determine the nature of the polythiophene-CeY composite formed when thiophene adsorbed on CeY from benzene solutions was used as the raw material. The FT-IR spectra of CeY and polythiophene-CeY composite are shown in **Figure 14**. The adsorbed water on CeY and thiophene-CeY gives rise to the peak around 1636 cm^{-1}, which is characteristic of bending vibrations of water molecules[45]. In the FT-IR spectrum of CeY zeolite, the band at 1036 cm^{-1} corresponds to the stretching vibrations of the Y zeolite structure framework[46], the peaks at 735 cm^{-1} and 581 cm^{-1} can be assigned to the Si-O-Si group in the CeY zeolite structure, and the band at 460 cm^{-1} is attributed to the bending vibrations of Si-O[47]. In the FT-IR spectrum of polythiophene-CeY, a band appears at 788 cm^{-1}, which can be assigned to C-H out-of-plane stretching vibrations. The presence of this band indicates that the polythiophene structure has been formed with α-α connection between

thiophene molecules[45, 48, 49]. The peaks at 1365 cm^{-1} and 1398 cm^{-1} can be assigned to C-H in-plane bending vibrations of thiophene molecules. The Si-O and Si-O-Si peaks of the CeY zeolite structure shift slightly in the polythiophene-CeY to 731 cm^{-1}, 578 cm^{-1} and 453 cm^{-1}. The shifts may be attributed to the chemical connection between polythiophene and CeY zeolite.

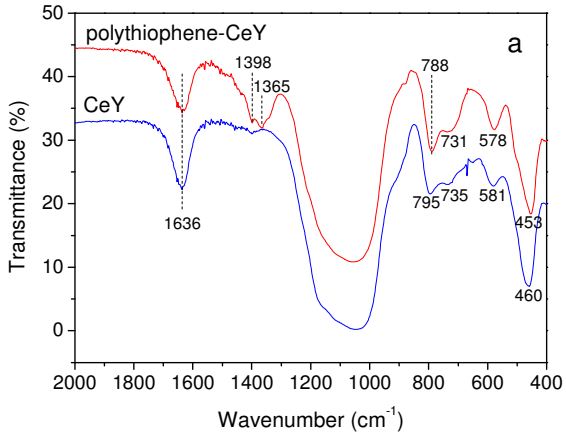

Figure 14. FT-IR spectra spectra of samples

In order to investigate whether the polythiophene-CeY composite still retained the structure of CeY zeolite, the XRD spectra of CeY sorbent, polythiophene and polythiophene-CeY prepared as above were measured (**Figure 15**). Clearly, both the polythiophene and the polythiophene in the polythiophene-CeY sample were non-crystalline, and the structure of the CeY zeolite was retained in the polythiophene-CeY materials, although the strength of the diffraction peaks decreased slightly.

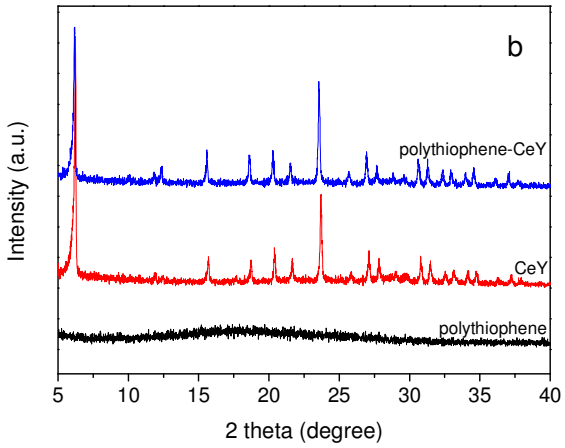

Figure 15. XRD spectra of samples

The change in the thermal stability of the polythiophene-CeY composite compared to polythiophene is shown by the TG and DTG curves (**Figure 16**). The single peak in the polythiophene DTG curve occurs at 420 °C, whereas there are two peaks in the polythiophene-CeY DTG curve, one at 79 °C (organic solution) and the other at 480 °C corresponding to the loss of polythiophene. Thus, the thermal stability of polythiophene was enhanced in the combination with CeY zeolite. This increase in stability may be due to the formation of specific sulfur-metal bonds between thiophene and Ce^{4+}, which would make the electrical cloud more uniform in density, and thus increase the resonance stability of the molecular bond and hence the thermal stability of the polythiophene in the polythiophene-CeY composite. The weight loss of the second step in the TG curve of polythiophene-CeY composite indicates that the mass fraction of polythiophene in the polythiophene-CeY material was about 21wt%.

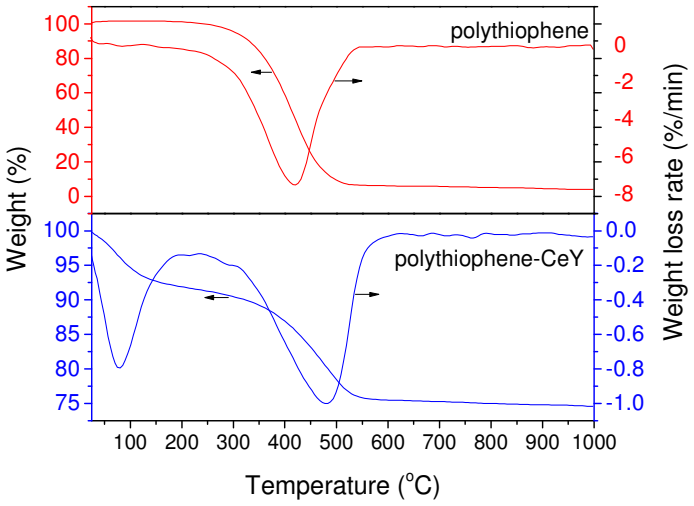

Figure 16. TG-DTG curves of polythiophene and polythiophene-CeY

3.3 Influence between one step and the next step in the process

In the whole explored process, it is probable that sodium hydroxide aqueous solution washing would affect the alkylation process carried with $AlCl_3$/silica gel as catalyst. In order to investigate it, 100 mL model coking benzene with thiophene, 1-hexene, and phenol concentration of 700 mg/L, 4200 mg/L and 5000 mg/L respectively was washed by 10 mL 30wt% sodium hydroxide aqueous solution in a flask under magnetic stirring at room temperature for 24 h. And then the mixture was put on a desk for 4 h to let the aqueous phase and organic phase separate by themselves, then the organic phase was separated by separatory funnel. After washing, the organic phase was determined by GC-FID and GC-FPD, and the results show that the phenol was almost completely removed and the concentration of thiophene and 1-exhene was 705.13 mg/L and 4214.26 mg/L respectively. Then the organic was used as the feedstock for the alkylation process as described in section 2.1, and the desulfurization results is shown in **Figure 17**. The washing process decreases the activity of $AlCl_3$/silica gel catalyst with the desulfurization efficiency of 85.1%. However, after the

organic product feedstock treated by 2 g anhydrous Na_2CO_3, the desulfurization efficiency is 91.7%, which was very close to 94.2% described in **Figure 8**. It means that the sodium hydroxide aqueous solution washing can bring light amount of water in the benzene solution, which is harmful to the activity of $AlCl_3$/silica gel catalyst.

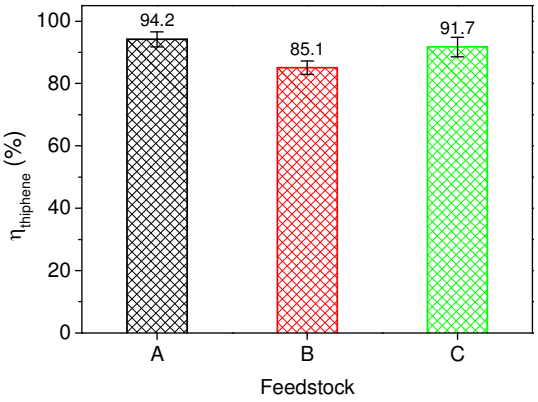

Figure 17. Effect of feedstock on thiophene conversion

(A was a result shown in **Figure 8**, B was the benzene solution after sodium hydroxide aqueous solution washing, C was prepared from B by anhydrous Na_2CO_3 dewatering)

In order to further understand this influence, different amount of water was added into the benzene solution described in section 2.1, and the desulfurization results were shown in **Figure 18**. With increasing of the water content in solution, thiphene conversion decreased, but it is still higher than 82.6% if the water content is not more than 1000 ppmw. This phenomenon should be caused by the reaction between the catalyst and water shown in **Figure 19**, because the reaction products do not have the alkylation activity.

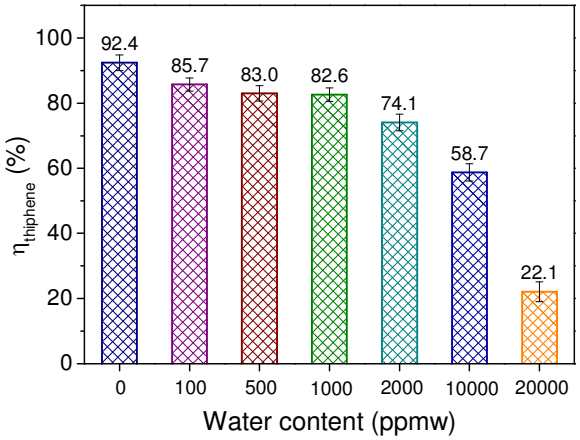

445

446 **Figure 18.** Influence of water on the conversion rate of thiophene

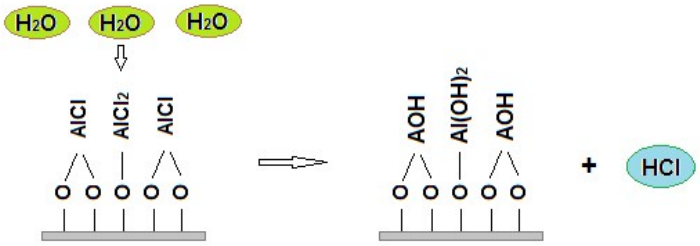

447

448 **Figure 19.** Scheme of the reaction between $AlCl_3$/silica gel catalyst and water

449 For the adsorption desulfurization process, the most probable influence factor from the
450 alkylation step is the changeable concentration of rest thiophene because the $AlCl_3$/silica gel
451 catalyst does not solve in benzene and the alkylthiopehenes are easily separated from benzene
452 by nowadays distillation technique due to their very different physical properties. In order to
453 investigate the influence of thiophene concentration on adsorption desulfurization step, the
454 breakthrough time vs thiophene concentration is shown in **Figure 20** and the adsorption
455 capacity vs thiophene concentration is shown in **Table 6**. CeY sorbent could almost
456 completely remove the thiophene from benzene when thiophene concentration is from 100
457 mg/L to 1000 mg/L. When the thiophene concentration decreased, the adsorption capacity
458 decreased, but the breakthrough time increased. The results indicated that this adsorption

method is most suitable for the desulfurization from low concentration sulfur-containing liquid because it can treat a relatively high amount of liquid. When the thiophene concentration was 100 mg/L, 12.04 mL no sulfur benzene could be obtained by using one gram of CeY sorbent, which was 3.56 times the amount of pure benzene obtained from 1000 mg/L thiophene-containing solution. The results mean that the catalytic process step and the adsorption step fit very well.

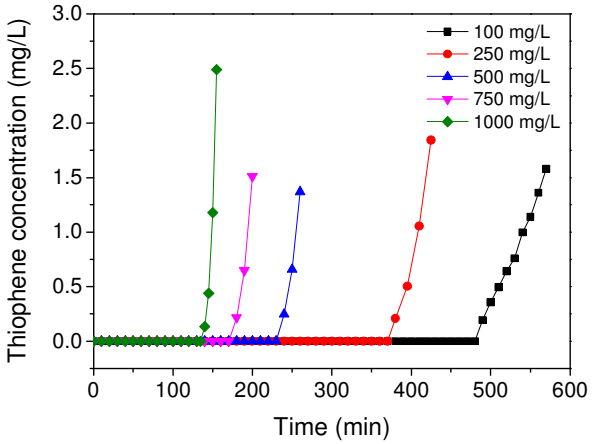

Figure 20. Breakthrough curves of CeY sorbent for different thiophene concentrations of the inlet solutions

(desulfurization temperature 22 °C, sorbent particle size of 0.2-0.3 mm, flow rate of 0.15 mL/min)

Table 6. Adsorption capacity of CeY sorbent for solutions with different concentrations of thiophene

Concentration of thiophene (mg/L)	100	250	500	750	1000
Q (mg/g)	1.20	2.31	2.88	3.20	3.38

3.4 Desulfurization mechanism of the process

In order to to give more details concerning to the process, the mechanism of the process is shown in **Figure 21** and **equations (7)** and **(8)**. In the pretreatment stage, the phenol, which is a weak acid, will form a salt with the strong base NaOH, and, since the salt is soluble in water, it will dissolve in the aqueous phase and be separated from benzene. The reaction equation is given below (**equation (7)**). In the first (□) stage, the thiophene is alkylated by the olefins in the presence of alkyl catalyst to give a substituted alkylthiophene, which has a very different boiling point from benzene and can therefore be easily separated from benzene by distillation. The alkylation equation is given as **equation (8)**. In the second (□) stage, the remaining thiophene is adsorbed by a sorbent by both physical and chemical adsorption processes. Finally (□), the sorbent after thiophene adsorption and the alkylthiophene are used to prepare the polythiophene-zeolite composite.

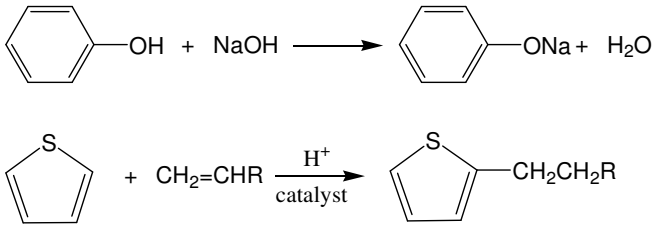

(7)

(8)

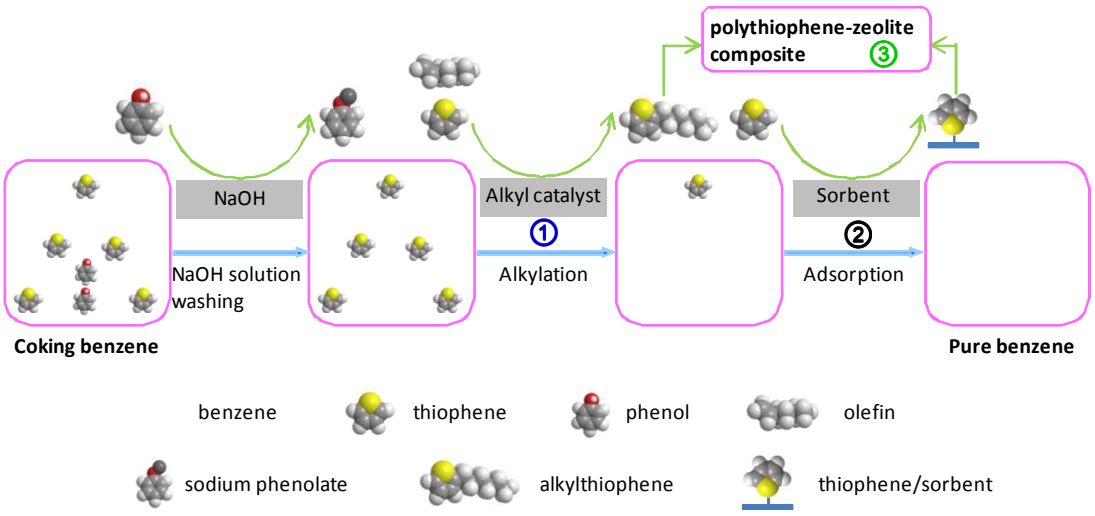

Figure 21. Mechanism of the process for desulfurization of coking benzene by a two-step method with reuse of sorbent/thiophene

To make the adsorption desulfurization more clear, the isothermal plot of thiophene capacity at 22 ℃ from **Table 6** is shown in **Figure 22a**, and the corresponding $\frac{C_{thiophene}}{Q}$ vs $C_{thiophene}$ plot, required to fit a Langmuir isotherm, is shown in **Figure 22b**. A very good linear fit (squared correlation coefficient 0.998) to the Langmuir equation, shown in **equations (5)** and **(6)**, was obtained.

$$Q = \frac{kQ_m C_{thiophene}}{1 + kC_{thiophene}} \quad (5)$$

$$\frac{C_{thiophene}}{Q} = \frac{1}{Q_m} C_{thiophene} + \frac{1}{kQ_m} \quad (6)$$

where, Q (mg/g) is the adsorption capacity; Q_m (mg/g) is the maximum adsorption capacity when the surface of sorbent is covered by a monolayer of thiophene; $C_{thiophene}$ (mg/L) is the concentration of thiophene in the solution; k is a constant. From the slope and intercept of the fitted line, Q_m=4.15 mg/g and k =0.077.

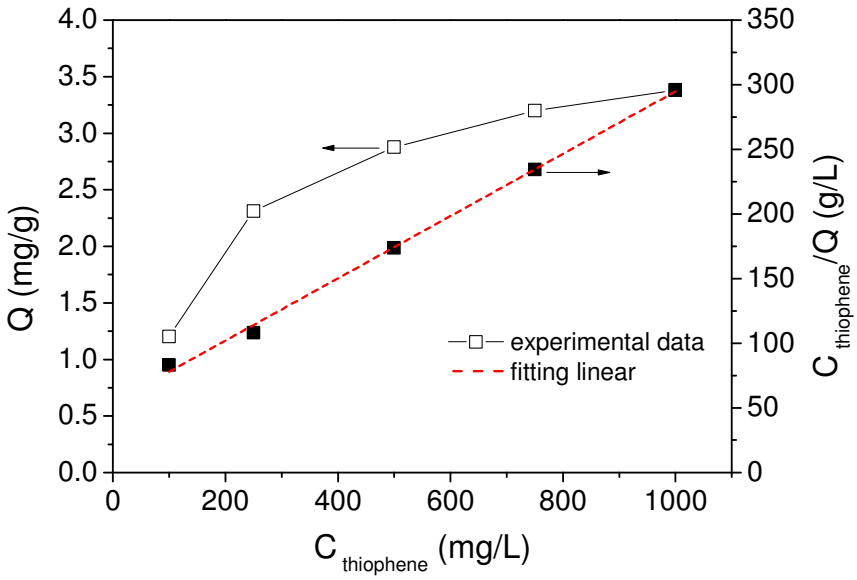

Figure 22. Adsorption isotherm of CeY at ambient temperature and the results fitted by Langmuir model

4. Conclusions

The $AlCl_3$/silica gel catalyst which was prepared in this work by a close pressurization method can effectively catalyze the alkylation of thiophene by olefins, desulfurization efficiency reaches up to 94.2 % of the thiophene in simulated impure benzene. The last traces of thiophene could be removed by adsorption on NaY zeolite exchanged with cerium. The benzene obtained would be sufficiently low in thiophene (< 0.01 ppm) to be used as a chemical feedstock. The CeY zeolite with adsorbed thiophene can be used to prepare a polythiophene-CeY composite. Thus the green process described in this paper can be used to refine coking benzene and desulfurize with the advantages of easy operation, low pollution and the additional advantages of reusing the thiophene and the used sorbent. Furthermore, the catalyst preparation was more rapid and energy efficient than previous methods, with no use of toxic solvents. The catalyst presented a high activity for the simultaneous alkylation removal of thiophene and olefin, which are present in coking benzene as impurities, and the sorbent for the finishing stage of thiophene removal was more efficient than sorbents previously used.

Acknowledgements

The authors gratefully acknowledge Dr. Marc Marshall in Monash University for comments and language revision on this paper, Mr. Wenbo Wang, Ms Yuanyuan Xie, and Mr Jinyu Chang for the XRD, FT-IR and TG characterization respectively. The financial support of National Natural Science Foundation of China (51242003, 51372161, 21406151), Research Fund for Doctoral Program of High Education (20131402110010) and Shanxi Scholarship Council of China (2012-0039) were highly appreciated.

References

1. M. C. Capel-Sanchez, J. M. Campos-Martin and J. L. G. Fierro, *Energy & Environmental Science*, 2010, **3**, 328-333.
2. F. Lin, D. Wang, Z. Jiang, Y. Ma, J. Li, R. Li and C. Li, *Energy & Environmental Science*, 2012, **5**, 6400-6406.
3. P. S. Kulkarni and C. A. M. Afonso, *Green Chemistry*, 2010, **12**, 1139-1149.
4. S. R. H. Barrett, S. H. L. Yim, C. K. Gilmore, L. T. Murray, S. R. Kuhn, A. P. K. Tai, R. M. Yantosca, D. W. Byun, F. Ngan, X. Li, J. I. Levy, A. Ashok, J. Koo, H. M. Wong, O. Dessens, S. Balasubramanian, G. G. Fleming, M. N. Pearlson, C. Wollersheim, R. Malina, S. Arunachalam, F. S. Binkowski, E. M. Leibensperger, D. J. Jacob, J. I. Hileman and I. A. Waitz, *Environmental Science & Technology*, 2012, **46**, 4275-4282.
5. T. V. Choudhary, S. Parrott and B. Johnson, *Environmental Science & Technology*, 2008, **42**, 1944-1947.
6. H. Fan, T. Sun, Y. Zhao, J. Shangguan and J. Lin, *Environmental Science & Technology*, 2013, **47**, 4859-4865.
7. J. Liao, W. Wang, H. Wang, Q. Jin and L. Chang, *Modern Chemical Industry*, 2009, **29**, 219-221.
8. R. Xiao and B. Jinfeng, *Coal Chemical Products and Technology*, Metallurgical Industry Press, 2008.
9. Y. Kim, S. Cook, S. M. Tuladhar, S. A. Choulis, J. Nelson, J. R. Durrant, D. D. C. Bradley, M. Giles, I. McCulloch, C. Ha and M. Ree, *Nat Mater*, 2006, **5**, 197-203.
10. S. D. Oosterhout, M. M. Wienk, S. S. van Bavel, R. Thiedmann, L. Jan Anton Koster, J. Gilot, J. Loos, V. Schmidt and R. A. J. Janssen, *Nat Mater*, 2009, **8**, 818-824.
11. J. Janata and M. Josowicz, *Nat Mater*, 2003, **2**, 19-24.
12. R. Capelli, S. Toffanin, G. Generali, H. Usta, A. Facchetti and M. Muccini, *Nat Mater*, 2010, **9**, 496-503.
13. T. L. Andrew, H. Tsai and R. Menon, *Science*, 2009, **324**, 917-921.
14. R. Österbacka, C. P. An, X. M. Jiang and Z. V. Vardeny, *Science*, 2000, **287**, 839-842.
15. M. Arvand, R. Ansari and L. Heydari, *Materials Science and Engineering: C*, 2011, **31**, 1398-1404.
16. N. Ballav and M. Biswas, *Materials Science and Engineering: B*, 2006, **129**, 270-272.
17. N. Ballav and M. Biswas, *Polymer International*, 2003, **52**, 179-184.
18. A. L. Briseno, T. W. Holcombe, A. I. Boukai, E. C. Garnett, S. W. Shelton, J. J. M. Fréchet and P. Yang, *Nano Letters*, 2010, **10**, 334-340.
19. Q. Pang, J. Han, C. Liang, L. Zhou and J. Luo, *Journal of Functional Materials*, 2010, **41**, 997-1000.
20. Z. Yang, X. Kou, W. Ni, Z. Sun, L. Li and J. Wang, *Chemistry of Materials*, 2007, **19**, 6222-6229.
21. H. Wang, S. Jin, G. Tang, F. Han, D. Liang and X. Xu, *Acta Chimica Sinica*, 2007, **65**, 2923-2928.
22. *United States Pat.,* 2707699, 1955.
23. *United States Pat.,* 3879268, 1975.
24. L. Cheng, *Shanxi Chemical Industry*, 2009, **29**, 1-3.
25. C. Song, *Catalysis Today*, 2003, **86**, 211-263.
26. J. Gislason, *Oil Gas J.*, 2001, **99**, 72-72.
27. W. Wang, L. Ma, J. Liao, Y. Xie, J. Chang and L. Chang, *Chinese Journal of Catalysis*, 2012, **33**, 323-329.
28. R. Cámera, R. Rimada, G. Romanelli, J. C. Autino and P. Vázquez, *Catalysis Today*, 2008, **133–135**, 822-827.
29. J. Liao, Y. Zhang, W. Wang, X. Li and L. Chang, Detection of Thiophene and CS_2 in Coking Benzene Using GC-FPD, 2011.
30. L. Li, G. Luo, X. Xu, R. Liao and J. Gao, *Journal of Petrochemical Universities*, 2006, **19**, 56-59.
31. J. Liao, W. Bao, Y. Chen, Y. Zhang and L. Chang, *Energy Sources, Part A: Recovery, Utilization, and*

Environmental Effects, 2012, **34**, 618-625.
32. X. Wang and G. Luo, *Chinese Journal of Catalysis*, 1996, **17**, 530-534.
33. G. Luo, X. Xu and Z. Tong, *Journal of Fuel Chemistry and Technology*, 1999, **27**, 476-480.
34. Y. Xie, J. Liao, W. Wang, W. Bao, Y. Chen and L. Chang, *Chemical Industry and Engineering Progress*, 2011, **30**, 49-52.
35. Y. Jiang, X. Meng, X. Zhang and B. Zong, *Petrochemical Techonology*, 2004, **33**, 122-125.
36. J. Liao, Y. Zhang, W. Wang, Y. Xie and L. Chang, *Adsorption*, 2012, **18**, 181-187.
37. J. Liao, L. Bao, W. Wang, Y. Xie, J. Chang, W. Bao and L. Chang, *Fuel Processing Technology*, 2014, **117**, 38-43.
38. Y. Shi, W. Zhang, H. Zhang, F. Tian, C. Jia and Y. Chen, *Fuel Processing Technology*, 2013, **110**, 24-32.
39. S. Sato, F. Nozaki, S. Zhang and P. Cheng, *Applied Catalysis A: General*, 1996, **143**, 271-281.
40. R. G. Pearson, *Journal of the American Chemical Society*, 1963, **85**, 3533-3539.
41. A. J. Hernández-Maldonado, F. H. Yang, G. Qi and R. T. Yang, *Applied Catalysis B: Environmental*, 2005, **56**, 111-126.
42. A. J. Hernández-Maldonado and R. T. Yang, *Industrial & Engineering Chemistry Research*, 2003, **42**, 123-129.
43. A. J. Hernández-Maldonado and R. T. Yang, *AIChE Journal*, 2004, **50**, 791-801.
44. X. Ju, H. Wang, J. Xu, L. Jin and L. Song, *Acta. Petrolei. Sinica. (Petroleum Processing Section)*, 2009, 655-660.
45. M. Lu and S. Yang, *Synthetic Metals*, 2005, **154**, 73-76.
46. L. Lin, Y. Zhang, H. Zhang and F. Lu, *Journal of Colloid and Interface Science*, 2011, **360**, 753-759.
47. R. Xu and W. Pang, *Zeolites and porous materials Chemistry*, Science Press, Beijing, 2004.
48. F. Han, D. Liang, H. Wang, G. Tang and X. Xu, *Journal of East China Normal University (Natural Science)* 2009, 129-135.
49. J. Roncali, *Chemical Reviews*, 1992, **92**, 711-738.